1064 nm laser-induced defects in pure SiO_2 fibers

J. M. Stone,* W. J. Wadsworth, and J. C. Knight

Centre for Photonics and Photonic Materials, Department of Physics, University of Bath, Bath BA2 7AY, UK
**Corresponding author: j.m.stone@bath.ac.uk*

Received April 11, 2013; revised June 6, 2013; accepted June 21, 2013;
posted June 25, 2013 (Doc. ID 188682); published July 23, 2013

We investigate evidence of the formation of nonbridging oxygen hole centers in pure silica photonic crystal fibers from 5 ps 1064 nm pulses. The formation of the defects is attributed to the breaking of stressed silicon–oxygen bonds in the glass matrix through a many-photon process. We compare the photodarkening induced by the 1064 nm pump with photodarkening induced by short wavelength light in a 1064 nm pumped supercontinuum extending to 400 nm. It is shown that the higher peak power at the pump wavelength makes it a more significant cause of photodarkening when compared to the shorter wavelength light generated in the fiber. © 2013 Optical Society of America

OCIS codes: (060.2290) Fiber materials; (060.4370) Nonlinear optics, fibers; (160.6030) Silica.
http://dx.doi.org/10.1364/OL.38.002717

Defects induced in glass by lasers, or by high-energy photons or particles, are particularly important due to the ubiquity of glass optical fibers. Defect creation has been widely explored in pure and doped silica (SiO_2), as silica is the most widely used glass for optical fibers [1,2]. These studies become even more valuable as fibers find their way into increasing numbers of critical applications and carry ever-higher optical powers. Frequently, induced defects manifest themselves as broad absorption bands in the visible and ultraviolet spectral regions, degrading optical fiber performance in these regions. When the defects are caused by light itself, this process is known as photodarkening. Perhaps the most frequently encountered defect is a partially bound oxygen atom with one free electron, the nonbridging oxygen hole center (NBOHC). The NBOHC has a strong absorption band at 258 nm wavelength and a weaker band at 630 nm, which although less than 3% of the strength of the 258 nm band, can create significant problems for the guidance of visible light in silica core optical fibers [1–3]. This defect commonly forms as a result of optically induced breaking of a bond in a stressed multiple member $(Si\text{-}O)_n$ ring. This damage also results in a dangling Si bond (absorbing at 213 nm) known as an E′ center. The stressed bonds which are the precursors to these sites result from three- or four-member ring structures in the silica matrix where the Si–O–Si bonds are not allowed to exist with their natural angle [4]. Previous work has shown that defects can be induced from stressed bonds through exposure to gamma rays [5,6] and high-energy particles [7] but also through one or two photon absorption occurring during the guidance of light from UV excimer lasers (KrF 248 m, ArF 193 nm, and F_2 157 nm) [8,9]. Other work has also been reported which demonstrates defect formation in bulk media due to few photon absorption from ultrashort, microjoule titanium sapphire laser pulses with high peak powers (50–300 MW) in the near infrared (800 nm) [10]. In order to produce fibers which do not suffer from such damage, various treatment techniques have been developed. These techniques typically involve hydrogen/deuterium loading [11,12], the use of fluorine-doped glass as a core material [13–16], or thermal annealing to relax the glass structure [9], although all of these processes are in essence methods of allowing the glass structure to relax. The introduction of fluorine as a dopant terminates stressed rings leading to a "C" shape rather than a ring, which also allows the structure to relax and enables a greater number of Si–O–Si bonds to have a natural angle. A similar beneficial effect is caused by OH groups in high water content fibers [4]; however, a high OH content is often undesirable due to the resulting spectral absorption in the near-IR. Molecular H_2 (or D_2) [17,18] can also be introduced to the glass under pressure so that once NBOHCs have been formed and the structure relaxed, the hydrogen/deuterium will readily react at the defect sites terminating them as Si–O–H [19]. This removes the 630 nm absorption of NBOHC, but of course leads to high near-IR absorption from O–H bonds, which can be shifted toward the mid-IR for O-D. It should be noted that photodarkening in ytterbium-doped fiber amplifiers is also a significant area of research due to the prominence of high power ytterbium fiber-based laser systems. Defect centers are similar to those in pure silica although the precursor sites, formation routes, and mitigation techniques are reported to differ [20,21].

It has been shown that NBOHC formation in pure silica is initiated by photon energies close to the fundamental absorption edge of silica at 8 eV (corresponding to approximately 160 nm wavelength) [8]. Due to this relatively high absorption energy, studies have principally focused on defects formed through exposure to gamma radiation and UV damage from one or two photon absorption. In this Letter, we study the relative contribution to photodarkening in supercontinuum fibers from the pump pulses and from the generated visible supercontinuum. We present evidence of significant NBOHC formation in all-silica optical fibers induced by an infrared 1064 nm (1.2 eV) source producing 5 ps pulses with submicrojoule pulse energies at peak powers of 10 s of kilowatts. We show that photodarkening in fiber-based supercontinuum sources is predominantly caused by many-photon absorption of pump light rather than by fewer-photon absorption of the internally generated visible light.

The pump source used in our experiments emits 5 ps, 1064 nm pulses at a repetition rate of 20 MHz. In our control experiments, to prevent the formation of optical

solitons and the resulting extreme spectral broadening (optical supercontinuum) [22,23], which could itself cause defect formation, a photonic crystal fiber with an all-normal dispersion profile (effective core area 7.1 μm^2) was used as a test fiber. This fiber was identical to that used by Hooper *et al.* [24]. The fiber was fabricated from pure silica (Heraeus F300) and spliced directly to our pump source. The fiber was unused before our experiments. Three 2 m lengths of fiber were tested in all, using three different output powers from the test fibers of 2.66, 2.15, and 1.67 W. These average powers for sech-squared pulses correspond to pulse energies of 133, 107, and 83 nJ and peak powers of 23.4, 18.9, and 14.7 kW, respectively. The output spectrum for the 2.66 W case is shown in Fig. 1(a). It can be seen that although there is significant nonlinear broadening to longer wavelengths, very little light is generated below the pump. Although Fig. 1(a) only shows the spectrum from 600 nm, no light was detected down to a wavelength of 200 nm. In each case, the laser was left to run for 24 h, after which the test fiber was removed and white light (tungsten bulb) transmission measurements were taken. The white light was coupled into each of the normal dispersion fibers from the output end, and in each case the transmitted spectrum was measured. The first 20 cm of each fiber, that is, the end which was previously spliced to the pump, was then cut off and the transmission was measured again, with this repeated in 20 cm lengths.

A second fiber was also tested, again fabricated from pure silica, however, with a high air filling fraction design which would allow supercontinuum generation via group index matching with a shortest wavelength of 400 nm from our 1064 nm pump (effective core area 11.6 μm^2) [25]. The fiber was identical to that in [25] except that the size of the holes on one of the fiber's axes was adjusted in order to give enhanced birefringence for other applications. This fiber was 10 m long and specifically tested in order to compare the effects of photodarkening from the pump light at the input end of the fiber with the effects of photodarkening arising from the short wavelength light generated in a supercontinuum and propagating toward the output end of the fiber. For the pump source used in our experiments, the shortest wavelengths were present after 2 m propagation, while the output spectrum after 10 m can be seen in Fig. 1(b). This fiber was run for 47 h. The output spectra at 0 and 47 h are both shown in Fig. 1(b); there is significantly less light in the visible part of the spectrum after 47 h illustrating how photodarkening can degrade visible light transmission in untreated optical fibers. Over 10 m of fiber, the loss at the longest wavelengths of the generated supercontinuum is significant due to strong OH absorption bands [26], so the total output power in the supercontinuum therefore in this case is not an accurate value of the input power. In order to gain an approximate value for the input power in our supercontinuum fiber, shorter sections of fiber (<2 m) were subsequently spliced to the pump, and the total output power measured on average to be 2.4 W. This value for average power gives an approximate input pulse energy of 120 nJ with a peak power of 21 kW. Cutbacks were made on the supercontinuum fiber in a similar way to the all-normal dispersion fiber, although 2 m rather than 20 cm sections were removed.

The losses in the 20 cm cutbacks on the all-normal dispersion fiber are shown in Figs. 2(a)–2(c). Figure 2(a) shows the cutbacks for the fiber run at the highest power, 2.66 W. The curves show the loss with each cutback. A large absorption band can be seen centered around 630 nm, a clear indication of NBOHCs. The maximum induced loss in the first 20 cm at 630 nm is 3.9 dB, with the loss in the subsequent 20 cm sections reducing as the peak power of the pulse is reduced largely due to the effects of self-steepening until there is negligible loss between 60 and 80 cm. The total induced loss in the removed 80 cm is in excess of 6 dB. This high loss toward the input of the fiber can only have been induced by the 1064 nm pump radiation, which would require seven photons to reach the 8 eV absorption edge. The results for lower input powers 2.15 and 1.67 W can be seen,

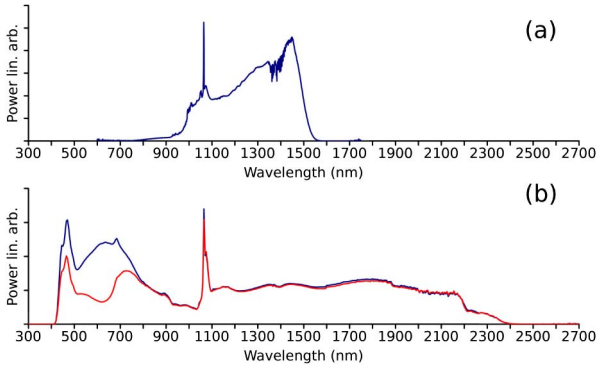

Fig. 1. (a) Output spectrum after 2 m of all normal dispersion fiber from our highest power (2.66 W) experiment. Although data are only presented to 600 nm, no light was detected down to 200 nm. (b) Output spectra at 0 and 47 h (shown in blue and red, respectively) after 10 m of supercontinuum fiber. Evidence of photodarkening can clearly be seen from the depletion of the visible region of the supercontinuum after 47 h.

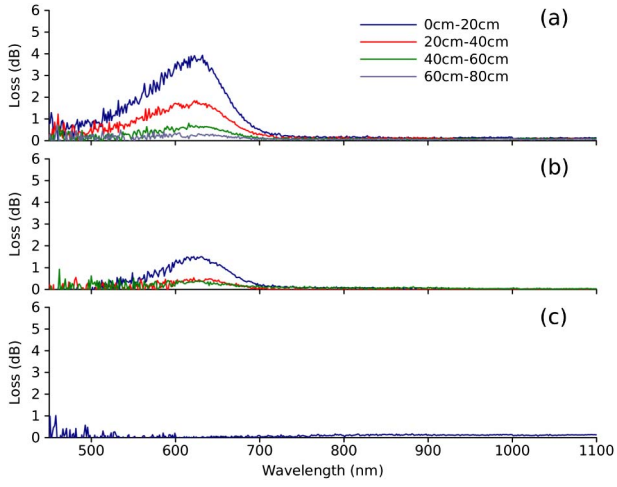

Fig. 2. Induced loss measured in 20 cm cutbacks of our all-normal dispersion fiber samples after 24 h. (a) is for an average output power during the experiment of 2.66 W, (b) is for 2.15 W, and (c) is for 1.67 W. The ordering of the legend reflects the order in which the traces appear in each plot at 630 nm. In (b) no trace is shown for 60–80 cm and in (c) only 0–20 cm is shown.

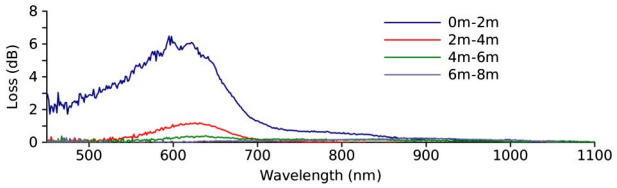

Fig. 3. Induced loss measured in 2 m cutbacks of our supercontinuum fiber after running for 47 h. The ordering of the legend reflects the order in which the traces appear at 630 nm.

respectively, in Figs. 2(b) and 2(c). For 2.15 W output power, the induced absorption at 630 nm is reduced, but the first 20 cm still contributes over half of the loss measured in the first 60 cm. Once the output power is reduced further to 1.67 W, no loss at 630 nm could be detected. The very steep power dependence of the loss is consistent with a highly multiphoton process.

Figure 3 shows the loss in the cutbacks from the 10 m section of supercontinuum fiber. Again the largest induced loss can be seen at the input end of the fiber, despite there being greater (average) power at short wavelengths toward the output end of the fiber. The initial 2 m section shows a broader loss band extending throughout the visible spectrum causing the significant depletion of the supercontinuum throughout this spectral region, which can be seen in Fig. 1(b). The depletion of the supercontinuum has predominantly occurred over the first 2 m where it is generated rather than the following 8 m where it is propagating with all the visible frequencies present down to 400 nm. This loss distribution shows clearly that the presence of visible light cannot be the sole cause of photodarkening in pure silica fibers. Direct comparison of the induced photodarkening in the two fibers shows that the induced photodarkening in the all-normal dispersion fiber, in which visible and ultraviolet light is never generated, is at least equal to that in the supercontinuum fiber which generates visible light. Our results clearly show that in the context of supercontinuum generation, the photoinduced attenuation due to defect formation can result more from direct many-photon absorption at the pump wavelength than from the absorption from fiber-generated visible and ultraviolet light.

We have observed the formation of NBOHC in pure silica photonic crystal fibers from 5 ps infrared pulses at 1064 nm. The formation has been attributed to the breaking of stressed silicon–oxygen bonds in the silica matrix via a many-photon process. In the context of supercontinuum generation, we have shown that the high peak power at the pump wavelength of 1064 nm is a more significant cause of photodarkening than the generation of short wavelength light down to 400 nm.

The authors would like to thank Dr. L. E. Hooper for providing the all-normal dispersion fiber.

References

1. L. Skuja, J. Non-Cryst. Solids **239**, 16 (1998).
2. L. Skuja, K. Kajihara, M. Hirano, and H. Hosono, Phys. Rev. B **84**, 205206 (2011).
3. H. Hosono, Y. Ikuta, T. Kinoshita, K. Kajihara, and M. Hirano, Phys. Rev. Lett. **87**, 175501 (2001).
4. F. L. Galeener, J. Non-Cryst. Solids **71**, 373 (1985).
5. K. Nagasawa, Y. Ohki, and Y. Hama, Jpn. J. Appl. Phys. **26**, L1009 (1987).
6. O. Deparis, D. Griscom, P. Mégret, M. Decréton, and M. Blondel, J. Non-Cryst. Solids **216**, 124 (1997).
7. D. L. Griscom, M. E. Gingerich, E. J. Friebele, M. Putnam, and W. Unruh, Appl. Opt. **33**, 1022 (1994).
8. K. Kajihara, L. Skuja, M. Hirano, and H. Hosono, Appl. Phys. Lett. **79**, 1757 (2001).
9. K. Kajihara, Y. Ikuta, M. Oto, M. Hirano, L. Skuja, and H. Hosono, Nucl. Instr. Methods B **218**, 323 (2004).
10. A. Zoubir, C. Rivero, R. Grodsky, K. Richardson, M. Richardson, T. Cardinal, and M. Couzi, Phys. Rev. B **73**, 224117 (2006).
11. K. Nagasawa, Y. Hoshi, Y. Ohki, and K. Yahagi, Jpn. J. Appl. Phys. **24**, 1224 (1985).
12. J. Stone, J. Lightwave Technol. **5**, 712 (1987).
13. H. Hosono, M. Mizuguchi, L. Skuja, and T. Ogawa, Opt. Lett. **24**, 1549 (1999).
14. H. Hosono and Y. Ikuta, Nucl. Instr. Methods B **166**, 691 (2000).
15. K. Saito and A. Ikushima, J. Appl. Phys. **91**, 4886 (2002).
16. M. Oto, S. Kikugawa, T. Miura, M. Hirano, and H. Hosono, J. Non-Cryst. Solids **349**, 133 (2004).
17. J. Stone and G. E. Walrafen, J. Chem. Phys. **76**, 1712 (1982).
18. J. Stone, Ind. Eng. Chem. Prod. Res. Dev. **25**, 609 (1986).
19. M. Vitiello, N. Lopez, F. Illas, and G. Pacchioni, J. Phys. Chem. A **104**, 4674 (2000).
20. S. Jetschke, S. Unger, A. Schwuchow, M. Leich, and J. Kirchhof, Opt. Express **16**, 15540 (2008).
21. M. Engholm, P. Jelger, F. Laurell, and L. Norin, Opt. Lett. **34**, 1285 (2009).
22. J. M. Dudley, G. Genty, and S. Coen, Rev. Mod. Phys. **78**, 1135 (2006).
23. A. V. Gorbach, D. V. Skryabin, J. M. Stone, and J. C. Knight, Opt. Express **14**, 9854 (2006).
24. L. E. Hooper, P. J. Mosley, A. C. Muir, W. J. Wadsworth, and J. C. Knight, Opt. Express **19**, 4902 (2011).
25. J. M. Stone and J. C. Knight, Opt. Express **16**, 2670 (2008).
26. O. Humbach, H. Fabian, U. Grzesik, U. Haken, and W. Heitmann, J. Non-Cryst. Solids **203**, 19 (1996).